1 **A T6SS in the coral pathogen *Vibrio coralliilyticus* secretes an arsenal**
2 **of anti-eukaryotic effectors and contributes to virulence**

3

4 **Short title:**

5 ***Vibrio coralliilyticus* T6SS effector repertoires**

6

7 Shir Mass[1], Hadar Cohen[1], Motti Gerlic[1], Blake Ushijima[2], Julia C. van Kessel[3], Eran Bosis[4], and
8 Dor Salomon[1,*]

9

10 [1] Department of Clinical Microbiology and Immunology, School of Medicine, Faculty of Medical
11 and Health Sciences, Tel Aviv University, Israel

12 [2] Department of Biology and Marine Biology, University of North Carolina Wilmington,
13 Wilmington, NC, USA

14 [3] Department of Biology, Indiana University, Bloomington, Indiana, USA

15 [4] Department of Biotechnology Engineering, Braude College of Engineering, Karmiel, Israel

16 [*] For correspondence: dorsalomon@mail.tau.ac.il

17

18 Keywords: T6SS, *Vibrio coralliilyticus*, *Artemia*, competition, virulence, effectors
19

20

Abstract

Vibrio coralliilyticus (*Vcor*) is a pathogen of coral and shellfish, leading to devastating economic and ecological consequences worldwide. Although rising ocean temperatures correlate with increased *Vcor* pathogenicity, the specific molecular mechanisms and determinants contributing to virulence remain poorly understood. Here, we systematically analyzed the type VI secretion system (T6SS), a contact-dependent toxin delivery apparatus, in *Vcor*. We identified two omnipresent T6SSs that are activated at temperatures in which *Vcor* becomes virulent; T6SS1 is an antibacterial system mediating interbacterial competition, whereas T6SS2 mediates anti-eukaryotic toxicity and contributes to mortality during infection of an aquatic model organism, *Artemia salina*. Using comparative proteomics, we identified the T6SS1 and T6SS2 toxin arsenals of three *Vcor* strains with distinct disease etiologies. Remarkably, T6SS2 secretes at least nine novel anti-eukaryotic toxins comprising core and accessory repertoires. We propose that T6SSs differently contribute to *Vcor*'s virulence: T6SS2 plays a direct role by targeting the host, while T6SS1 plays an indirect role by eliminating competitors.

Author Summary

Coral reefs are diverse ecosystems providing habitats for various fish, invertebrates, and microorganisms. Climate change, leading to rising ocean water temperatures, correlates with coral bleaching and mass mortality events. An implicated causal agent of coral disease outbreaks is the marine bacterium *Vibrio coralliilyticus*. Here, we found that two toxin injection systems present in all *Vibrio coralliilyticus* strains are regulated by temperature; we revealed the toxins that they secrete and their function in competition against rival bacteria and in the intoxication of an animal host. Our findings implicate these systems as previously unappreciated contributors to *Vibrio coralliilyticus* virulence, illuminating possible targets to treat or prevent coral infection.

Introduction

The oceans are home to Gram-negative marine bacteria of the genus *Vibrio*. These include many established and emerging pathogens that infect humans and marine animals [1,2]. In the past, vibrios were primarily associated with the warmer equatorial waters. Yet, in recent decades, they have spread to other regions, including the northern USA, Canada, and North Europe [3,4]. This spread correlates with rising ocean surface-level temperatures and disease outbreaks [5,6].

Corals are marine animals affected by rising ocean temperatures caused by climate change and the spread of vibrios [7–9]. They are ecologically and economically important because they provide diverse ecosystems used as habitats for various fish and invertebrates, as well as helping to protect shorelines from storm surges and erosion [10]. The coral animal lives in a symbiotic relationship with photosynthetic endosymbiotic dinoflagellates and microbes (collectively called the coral holobiont) [11–14]. *Vibrio coralliilyticus* (*Vcor*) is a bacterial pathogen shown to be a cause of diseases resulting in bleaching or tissue loss in corals [9,15,16]. Among other coral pathogens [9], *Vcor* stands out due to its wide geographic spread and broad range of reported hosts. Aside from corals, *Vcor* is also responsible for mortalities in shellfish hatcheries [17].

The coral holobiont is affected by various environmental conditions, such as shifts in water temperature, pH, and nutrients. Elevated temperature is a key factor in many *Vcor* infections because it increases the abundance and virulence of many *Vcor* strains [14]. At temperatures below 23°C, *Vcor* strains are predominantly not pathogenic [8]. However, the virulence of many strains increases when temperatures rise above 23°C [14,15,18]. In some cases, the symbiotic dinoflagellates are killed, and coral bleaching occurs. With most pathogenic strains, shifts to >27°C result in coral tissue lysis and increased coral mortality [15]. Elevated temperatures are associated with the production of proteases and hemolysins, motility, antimicrobial resistance, and secretion systems in *Vcor* [19]. In addition, the expression of *toxR*, a transcription regulator associated with virulence in other vibrios [20], correlates with increased temperature and was shown to contribute to *Vcor* virulence [21]. These data provide strong evidence that temperature regulates virulence-associated genes in *Vcor*. Nevertheless, it remains unclear how these factors contribute to pathogenicity and whether the same factors play a role in virulence towards different hosts.

Many vibrios employ a specialized toxin delivery mechanism, the type VI secretion system (T6SS), to manipulate their environment [22–29]. The T6SS is a proteinaceous apparatus that is assembled inside the bacterial cell: a sheath structure engulfs an inner tube made of stacked hexameric rings of Hcp proteins, which is capped by a spike comprising a VgrG trimer sharpened by a PAAR repeat-containing protein (hereafter referred to as PAAR) [30]. This tube-spike complex is decorated with toxic proteins, called effectors, that mediate the toxic activities of the T6SS [31–33]. Contraction of the sheath propels the tube-spike complex out of the cell, providing it with sufficient force to penetrate the membrane of a neighboring cell where effectors are deployed [34]. Whereas most T6SSs investigated to date mediate interbacterial competitions by delivering antibacterial effectors, a few T6SSs have been shown to target eukaryotes and mediate virulence [33,35,36]. In accordance, although most *Vibrio* T6SSs play a role in interbacterial competitions [24–28,37–39], we and others recently revealed *Vibrio* T6SSs and effectors that target eukaryotes, and we postulated that they play a role in virulence [22,40–43].

Several studies reported the temperature-dependent expression of T6SS components in *Vcor* [19,42], suggesting that T6SSs play a role in the temperature-regulated transition to a pathogenic lifestyle. The antibacterial activity of one T6SS was previously demonstrated in two

3

94   *Vcor* strains [42,44]. However, the presence of other T6SSs in the *Vcor* pan-genome, their role,
95   regulation, effector repertoire, and contribution to virulence remain unknown. Here, we
96   systematically analyzed the T6SSs in the *Vcor* pan-genome and revealed two omnipresent
97   systems. Using three *Vcor* strains as model systems, we experimentally defined the
98   environmental conditions regulating the activation of these two T6SSs. We also identified their
99   function and effector repertoires. Importantly, we revealed nine novel anti-eukaryotic effectors
100   delivered by the *Vcor* T6SS2, contributing to *Vcor* virulence.

101

Results

103   *Two T6SSs are omnipresent in Vibrio coralliilyticus strains*

104   To identify the T6SSs found in the pan-genome of *Vibrio coralliilyticus* (*Vcor*), we retrieved the
105   sequences of the core T6SS sheath component, TssB, from 31 available RefSeq *Vcor* genomes
106   (**Dataset S1**) and analyzed their genomic neighborhoods. Our analyses revealed that all
107   genomes harbor two conserved T6SSs, named T6SS1 and T6SS2 (**Fig. 1** and **Dataset S2**),
108   suggesting that these T6SSs play an important role in the *Vcor* lifestyle. T6SS1 is similar to the
109   previously investigated T6SS1 from *V. parahaemolyticus* [24,45], *V. alginolyticus* [26], and *V.*
110   *proteolyticus* [28], sharing the same gene content and organization. We recently showed that
111   this system mediates interbacterial competition in the *Vcor* type strain BAA-450 and in strain
112   OCN008 [42,44]. Two additional T6SSs, which we named T6SS3 and T6SS4, are each found in
113   a single *Vcor* genome (**Dataset S2**). Notably, two genes encoding structural core components in
114   T6SS4 appear to include frameshifts, and the gene cluster lacks a gene encoding the
115   conserved T6SS core component, TssH (**Fig. 1**). Therefore, it is possible that T6SS4 is not
116   functional.
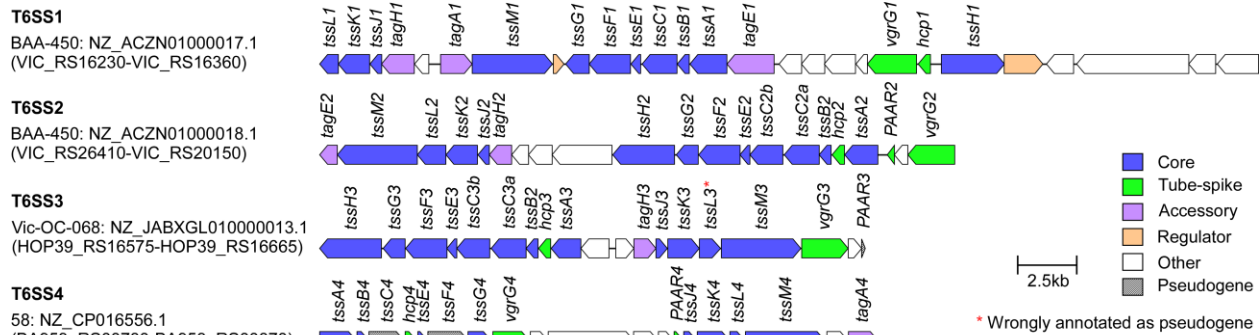
Fig. 1. Representative T6SS gene clusters found in *Vibrio coralliilyticus* genomes. The
strain name, GenBank accession number, and the first and last locus tag are denoted on the
left. Genes are denoted by arrows indicating the predicted direction of transcription. Encoded
proteins or domains are denoted above the genes.

121

122   *Environmental conditions regulate Vibrio coralliilyticus T6SSs*

123   Because T6SS1 and T6SS2 are omnipresent in *Vcor*, we set out to investigate their activation
124   and function. First, we sought to determine whether T6SS1 and T6SS2 are regulated by
125   environmental conditions regulating *Vcor* virulence. To this end, we selected three
126   representative *Vcor* strains harboring both T6SSs: BAA-450 (the type strain), OCN008, and
127   OCN014. These strains were isolated from different coral hosts and display different disease
128   etiologies [16,46,47]. Strains BAA-450 and OCN014 have a temperature-dependent infection

4

129 mode, and they become more virulent as temperatures rise above 23°C; the virulence of strain
130 OCN008 does not significantly change from 23 - 27°C [16,18,21].

131 To determine whether the activation of T6SS1 and T6SS2 depends on temperature or nutrient
132 availability, we monitored the expression and secretion of the conserved secreted T6SS
133 structural components, VgrG1 and Hcp2 [23], respectively. Bacteria were grown in either rich
134 (marine LB; MLB) or poor (glycerol artificial sea water; GASW) media and under a range of
135 physiologically relevant temperatures that affect *Vcor* pathogenicity: 19, 23, 28, and 31°C
136 [16,21,46]. As shown in **Fig. 2A-B**, we found that the activity of both T6SS1 and T6SS2 is
137 temperature- and media-dependent. In rich media, both systems are active between 23-31°C;
138 T6SS1 secretion peaks at 28°C, whereas T6SS2 secretion peaks at 31°C (**Fig. 2A**). Notably,
139 secretion via T6SS1 in strain OCN008 appears lower than in BAA-450 and OCN014. In poor
140 media, T6SS1 secretion peaks at 23°C in all strains and is retained at higher temperatures only
141 in strain BAA-450 (**Fig. 2B**); T6SS2 secretion is only observed in strain BAA-450 at 23°C.
142 Comparison between the activity of both systems in rich and poor media at 28°C revealed
143 higher levels of secretion in rich media (**Fig. 2C**). Therefore, unless otherwise indicated, we
144 performed subsequent analyses of T6SS1 and T6SS2 when *Vcor* strains are grown in rich
145 media at 28°C, conditions in which both systems are active in all three strains.
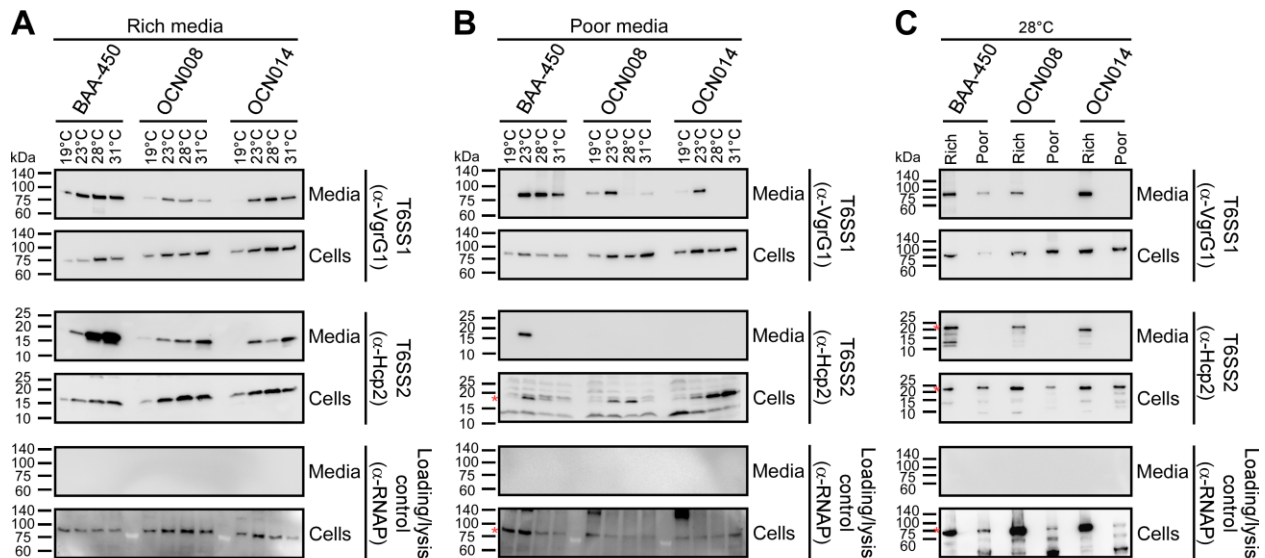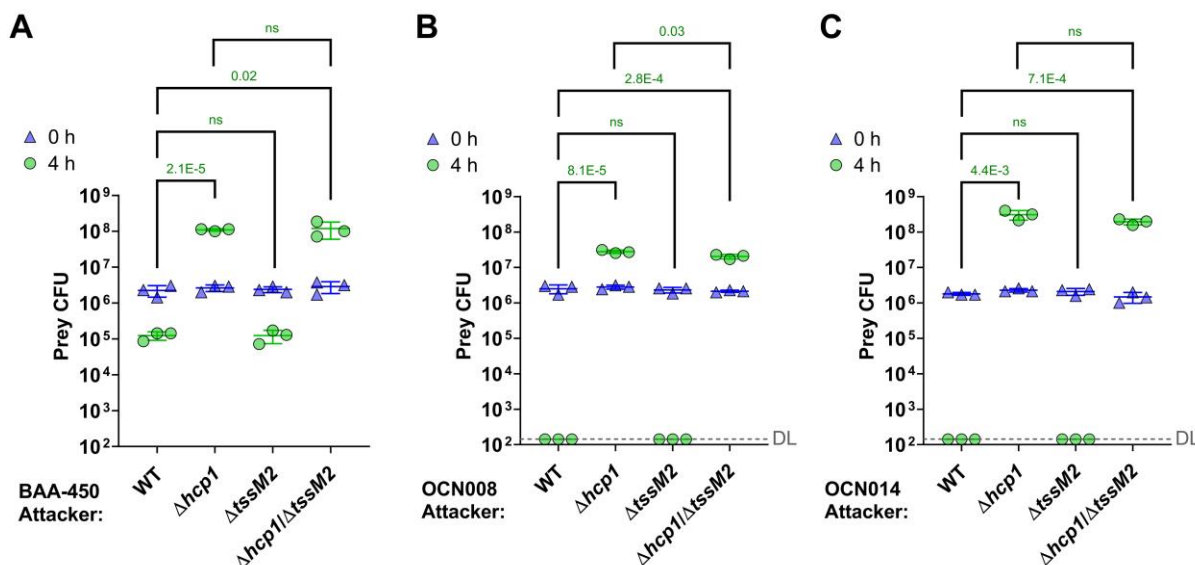

146 **Fig. 2. *Vibrio coralliilyticus* T6SS1 and T6SS2 are regulated by environmental conditions.**
147 Expression (cells) and secretion (media) of VgrG1 and Hcp2 from the three indicated *Vcor*
148 strains grown for 4 hours at the indicated temperatures in "rich" marine LB medium **(A)** or "poor"
149 glycerol artificial sea water medium **(B)**. **C)** Comparison of VgrG1 and Hcp2 expression and
150 secretion when *Vcor* strains were grown at 28°C in "rich" or "poor" media. RNA polymerase
151 sigma 70 (RNAp) was used as a loading and lysis control. Asterisks denote expected protein
152 sizes. Results from a representative experiment out of at least three independent experiments
153 are shown.

154

155 *T6SS1 mediates interbacterial competitions*

156 We previously reported that T6SS1 in strains BAA-450 and OCN008 mediates antibacterial
157 activity during interbacterial competitions [42,44]. To determine whether this is also true for
158 T6SS1 in strain OCN014 and whether T6SS2 also plays a role in interbacterial competition, we

5

159 set out to monitor the outcome of interbacterial competitions using *Vcor* strains in which the two
160 T6SSs were inactivated, either individually or together. To this end, we first constructed *Vcor*
161 mutant strains in which we inactivated T6SS1 by deleting the gene encoding the conserved
162 structural component Hcp1 (Δ*hcp1*), and T6SS2 by deleting the gene encoding the conserved
163 structural component TssM2 (Δ*tssM2*) (**Fig. S1A**). These mutations did not affect bacterial
164 growth (**Fig. S1B**). When competed against a sensitive a *V. natriegens* prey strain on rich media
165 plates at 28°C, all three *Vcor* strains killed the prey, evident by the decrease in prey viability
166 during the four hours of co-incubation with the wild-type *Vcor* attackers (**Fig. 3A-C**). This killing
167 was dependent on T6SS1, since its inactivation in the attacker strains by deleting *hcp1*
168 abolished the toxicity. Inactivation of T6SS2 by deleting *tssM2*, either alone or in combination
169 with an inactive T6SS1, had no effect on the observed antibacterial activity of *Vcor*. Taken
170 together, our results confirm that the *Vcor* T6SS1 mediates antibacterial activity and suggest
171 that T6SS2 does not play a role in interbacterial competition.
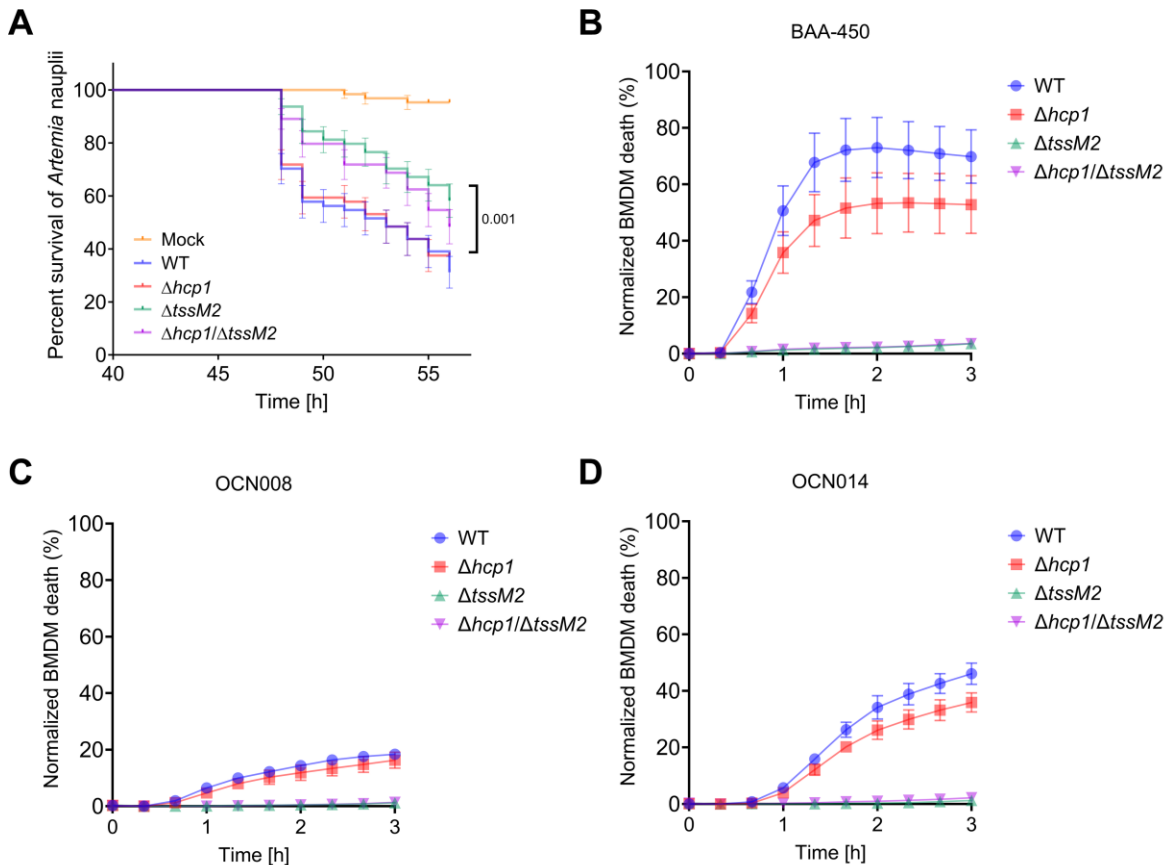

172 **Fig. 3. *Vibrio coralliilyticus* T6SS1 mediates interbacterial competition. A-C)** Viability
173 counts (colony forming units; CFU) of *V. natriegens* prey strains before (0 h) and after (4 h) co-
174 incubation with the indicated *Vcor* BAA-450 (A), OCN008 (B), or OCN014 (C) attacker strains
175 on MLB plates at 28°C. The statistical significance between samples at the 4 h time point was
176 calculated using an unpaired, two-tailed Student's *t* test; ns, no significant difference ($P > 0.05$);
177 WT, wild-type; DL, the assay's detection limit. Data are shown as the mean ± SD; $n = 3$. The
178 data shown are a representative experiment out of at least three independent experiments.

179

T6SS2 targets eukaryotes

181 Based on the above results, we hypothesized that T6SS2 mediates anti-eukaryotic activities. To
182 investigate whether T6SS2 plays a role in bacterial virulence, we employed the saline lake-
183 dwelling brine shrimp, *Artemia salina*, as an aquatic animal model [41,48,49]. Wild-type *Vcor*
184 OCN008 was lethal to *Artemia* nauplii (larvae), with a median survival of 53 hours. Inactivation
185 of T6SS2, either alone (Δ*tssM2*) or together with T6SS1 (Δ*hcp1*/Δ*tssM2*), resulted in a
186 significantly reduced lethality (median survival undefined or 56 hours, respectively), whereas
187 inactivation of T6SS1 (Δ*hcp1*) had no effect (**Fig. 4A**). These results reveal a role for the *Vcor*
188 T6SS2 in pathogenicity during infection of a eukaryotic host.

6

189   To further investigate the anti-eukaryotic activity of *Vcor* T6SS2 in all three strains, we used real-
190   time microscopy to monitor *Vcor*-mediated cell death kinetics. To this end, we employed bone
191   marrow-derived macrophages (BMDMs), which have been previously used as a model to
192   monitor the toxic effects of another *Vibrio* T6SS [40]. Various levels of cell death were observed
193   starting ~30 minutes after adding either of the wild-type *Vcor* strains BAA-450, OCN008, or
194   OCN014 (**Fig. 4B-D**). Remarkably, inactivation of T6SS2, either alone (Δ*tssM2*) or together with
195   T6SS1 (Δ*hcp1*/Δ*tssM2*), completely abrogated the *Vcor*-mediated cell death, whereas
196   inactivation of T6SS1 (Δ*hcp1*) had no or mild effect. These results support our hypothesis that
197   *Vcor* T6SS2 targets eukaryotes.

Fig. 4. ***Vibrio coralliilyticus* T6SS2 mediates lethality in *Artemia* nauplii and in**
macrophages. A) *Artemia* nauplii were challenged with the indicated *Vcor* OCN008 strains, and
survival was assessed 40 to 56 hours post-infection. Approximately 5×10^7 bacteria were added
to each well containing 2 nauplii. Data are shown as the mean ± SE of four biological replicates,
each comprising 16 nauplii for every bacterial strain. The statistical significance between the WT
and Δ*tssM2* curves was calculated using the Log-rank (Mantel-Cox) test. **B-D)** Assessment of
cell death upon infection of bone marrow-derived macrophages (BMDMs) with the indicated
Vcor BAA-450 (B), OCN008 (C), or OCN014 (D) strains. Approximately 3.5×10^4 BMDMs were
seeded into 96-well plates in triplicates and infected with *Vcor* strains at a multiplicity of infection
(MOI) ~ 4. Propidium iodide (PI) was added to the medium prior to infection, and its uptake
kinetics were assessed using real-time microscopy. WT, wild-type. Results from a representative
experiment out of at least three independent experiments are shown in B-D.

7

211 *T6SS1 and T6SS2 secrete diverse effector arsenals*

212 Next, we performed comparative proteomics analyses to reveal the *Vcor* T6SS secretomes and
213 identify the effectors that mediate the antibacterial and anti-eukaryotic activities described
214 above. Using mass spectrometry, we compared the proteins secreted by the wild-type *Vcor*
215 strains BAA-450, OCN008, and OCN014 with those secreted by their isogenic mutants in which
216 either T6SS1 or T6SS2 have been inactivated (Δ*hcp1* or Δ*tssM2*, respectively).

217 <u>T6SS1 secretomes:</u> We identified eleven, six, and eleven proteins that were significantly
218 enriched in the secretomes of wild-type strains BAA-450, OCN008, and OCN014, respectively,
219 compared to their T6SS1⁻ (Δ*hcp1*) mutants (**Fig. 5**, **Table 1**, and **Dataset S3-S5**). These include
220 the secreted tube-spike structural components Hcp1 (which was deleted to inactivate T6SS1),
221 VgrG1, and PAAR-like proteins. Most of the additional proteins are predicted antibacterial or
222 anti-eukaryotic effectors, or proteins encoded next to them, including: (i) homologs of previously
223 described T6SS effectors, with predicted toxic domains that target the peptidoglycan (e.g.,
224 WP_006961156.1 and WP_006961879.1); (ii) proteins containing MIX domains, which are
225 markers for T6SS effectors [45], with predicted nuclease or pore-forming toxic domains (e.g.,
226 WP_039951132.1 and WP_201765497.1); and (iii) proteins that have yet to be described as
227 related to T6SSs, which were identified only in the T6SS1 secretome of strain OCN008 (e.g.,
228 WP_021456284.1 and WP_021455387.1, which is a DEAD/DEAH box helicase). In accordance
229 with our observation that the T6SS1 appears less active in strain OCN008 compared to the two
230 other *Vcor* strains under the assay conditions (**Fig. 2A**), the comparative proteomics intensity
231 difference for the putative OCN008 T6SS1 effectors was low (**Fig. 5B**), suggesting that the latter
232 type of proteins detected only in the OCN008 T6SS1 secretome may be false positives. As
233 previously reported for similar T6SSs in other vibrios [26,28,45,50], some of the identified
234 proteins are encoded within the T6SS1 gene cluster, whereas others are encoded in auxiliary or
235 orphan operons. Moreover, predicted antibacterial effectors are encoded next to putative
236 immunity genes. Taken together, these results support our findings that *Vcor* T6SS1 plays a role
237 in interbacterial competitions using antibacterial effectors. Interestingly, in each *Vcor* strain, we
238 also identified a secreted MIX domain-containing effector that we previously showed or
239 hypothesized targets eukaryotes rather than bacteria (e.g., WP_006962196.1) [22]. This finding
240 suggests that T6SS1 also plays a role in interactions with eukaryotes, even though our
241 experiments did not reveal significant T6SS1-mediated anti-eukaryotic effects.
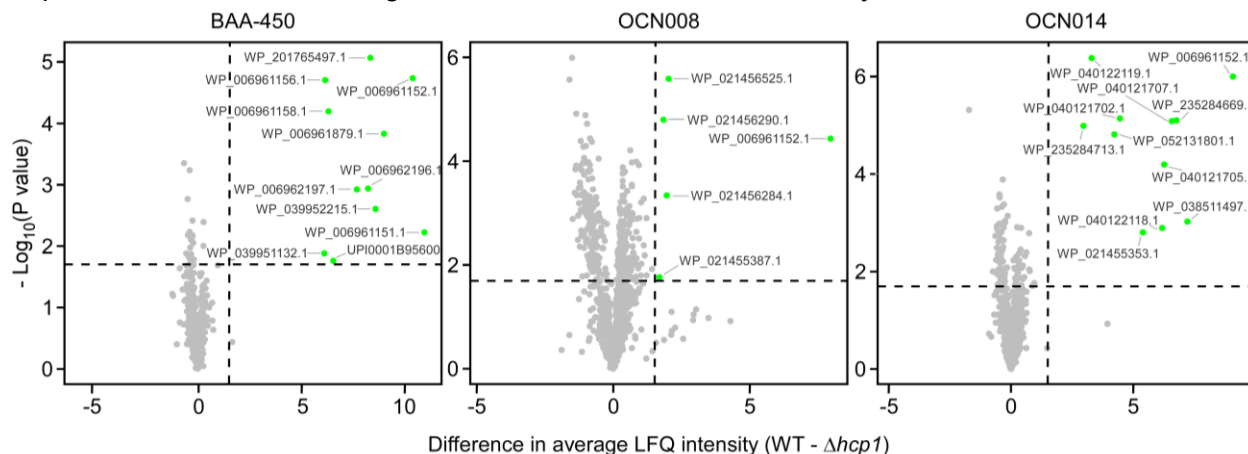
242 **Fig. 5. *Vibrio coralliilyticus* T6SS1 effector repertoires.** Volcano plots summarizing the
243 comparative proteomics of proteins identified in the media of the three indicated *Vcor* strains
244 with an active T6SS1 (WT, wild-type) or an inactive T6SS1 (Δ*hcp1*), using label-free
245 quantification (LFQ). The average LFQ signal intensity difference between the WT and Δ*hcp1*
246 strains is plotted against the -Log₁₀ of Student's *t* test *P* values (*n* = 3 biological replicates).

8

247 Proteins that were significantly more abundant in the secretome of the WT strains (difference in
248 average LFQ intensities > 1.6; *P* value < 0.02; with a minimum of two Razor unique peptides
249 and Score > 15) are denoted in green.

250

251 **Table 1. *Vibrio coralliilyticus* T6SS1 secretomes identified by comparative proteomics**

Predicted role	Predicted activity or domain	BAA-450		OCN008		OCN014	
		Protein accession	Gene locus	Protein accession	Gene locus	Protein accession	Gene locus
T6SS structural	Hcp	WP_006961152.1	VIC_RS16330	WP_006961152.1	G3U99_RS23805	WP_006961152.1	JV59_RS20030
	VgrG	WP_006961151.1	VIC_RS16325	N/D	N/D	WP_040121702.1	JV59_RS20025
	PAAR-like (DUF4150)	WP_039952215.1	VIC_RS19185	N/D	N/D	WP_040122118.1	JV59_RS22990
	PAAR-like (DUF4150)	UPI0001B95600 (annotated as a pseudogene in RefSeq)	VIC_RS08805	WP_021455353.1	G3U99_RS15395	WP_021455353.1	JV59_RS10110
Antibacterial effector	VP1390-like	WP_006961156.1	VIC_RS16350	WP_021456525.1	G3U99_RS23785	WP_040121705.1	JV59_RS20045
	Lysozyme-like	WP_006961879.1	VIC_RS19190	N/A	N/A	WP_040122119.1	JV59_RS22995
	MIX domain; TMs	WP_201765497.1	VIC_RS12080	N/D	N/D	WP_235284713.1	JV59_RS24085
	MIX domain; Pyocin_S; Colicin E9-like nuclease	WP_039951132.1	VIC_RS01010	N/A	N/A	N/A	N/A
	MIX domain; Colicin A-like pore-forming	N/A	N/A	N/A	N/A	WP_052131801.1	JV59_RS24930
	Unknown	N/A	N/A	WP_021456284.1	G3U99_RS12660	N/A	N/A
Anti-eukaryotic effector	MIX domain	WP_006962196.1	VIC_RS20535	N/A	N/A	N/A	N/A
	MIX domain	N/A	N/A	WP_021456290.1	G3U99_RS26335	WP_235284669.1	JV59_RS27320
Effector accessory	MIX domain-containing co-effector	WP_006961158.1	VIC_RS16360	N/D	N/D	WP_040121707.1	JV59_RS20055
	Encoded upstream of anti-eukaryotic MIX domain-containing effector	WP_006962197.1	VIC_RS20540	N/D	N/D	WP_038511497.1	JV59_RS07245
Unknown	DEAD/DEAH box helicase	N/D	N/D	WP_021455387.1	G3U99_RS17670	N/A	N/A

252 N/A, no homolog is encoded in the genome; N/D, a homolog is encoded in the genome but not detected in the mass-
253 spectrometry analysis; TM, transmembrane helix (according to phobius)

254

255 <u>T6SS2 secretomes:</u> We identified ten, nine, and six proteins that were significantly enriched in
256 the secretomes of wild-type strains BAA-450, OCN008, and OCN014, respectively, compared to
257 their T6SS2⁻ (Δ*tssM2*) mutants (**Fig. 6**, **Table 2**, and **Dataset S3-S5**). These include the
258 secreted tube-spike structural components Hcp2 and VgrG2. We predict that all the other
259 identified, non-structural proteins, which are encoded outside the T6SS2 gene cluster (**Fig. S2**),
260 are novel anti-eukaryotic effectors (excluding the phage shock protein, WP_021456780.1, which
261 is probably a phage protein and not a T6SS effector). In support of this prediction, none of these
262 proteins is encoded next to a gene that could encode for a cognate immunity protein. Moreover,
263 some are similar to previously described virulence toxins, such as WP_006960006.1 containing
264 a predicted YopT-like cysteine protease domain (YopT is a type III secretion system virulence
265 effector from *Yersinia* [51]). No putative effectors have a predicted signal peptide for the Sec or
266 Tat secretion systems that could account for their secretion, according to SignalP 6.0 [52]
267 analyses.

9
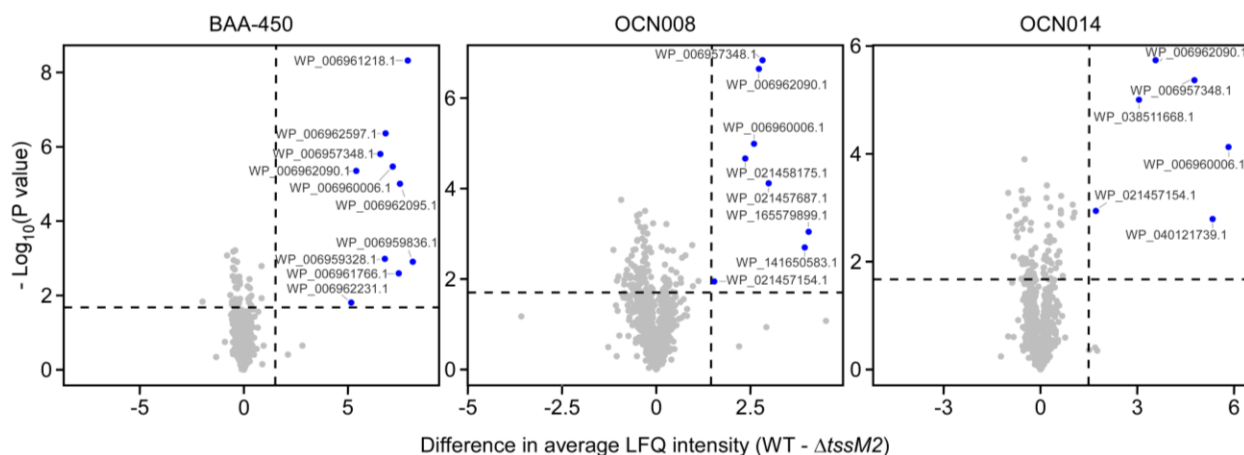
Fig. 6. *Vibrio coralliilyticus* T6SS2 effector repertoires. Volcano plots summarizing the comparative proteomics of proteins identified in the media of the three indicated *Vcor* strains with an active T6SS2 (WT, wild-type) or an inactive T6SS2 ($\Delta tssM2$), using label-free quantification (LFQ). The average LFQ signal intensity difference between the WT and $\Delta tssM2$ strains is plotted against the -$\log_{10}$ of Student's *t* test *P* values (*n* = 3 biological replicates). Proteins that were significantly more abundant in the secretome of the WT strains (difference in average LFQ intensities > 1.6; *P* value < 0.02; with a minimum of two Razor unique peptides and Score > 15) are denoted in blue.

Table 2. *Vibrio coralliilyticus* T6SS2 secretomes identified by comparative proteomics

Predicted role	Predicted activity or domain	BAA-450		OCN008		OCN014	
		Protein accession	Gene locus	Protein accession	Gene locus	Protein accession	Gene locus
T6SS structural	Hcp	WP_006962090.1	VIC_RS20130	WP_006962090.1	G3U99_RS13135	WP_006962090.1	JV59_RS07745
	VgrG	WP_006962095.1	VIC_RS20150	WP_021458175.1	G3U99_RS13110	WP_038511668.1	JV59_RS07720
Anti-eukaryotic effector	CNF-like [a] (CoVe1)	WP_006957348.1	VIC_RS01360	WP_006957348.1	G3U99_RS07885	WP_006957348.1	JV59_RS02730
	(p)ppGpp synthetase / hydrolase [a] (CoVe2)	WP_006959328.1	VIC_RS09310	WP_021457154.1	G3U99_RS15865	WP_021457154.1	JV59_RS10570
	Cysteine peptidase [a] (CoVe3)	WP_006959836.1	VIC_RS11210	N/D	N/D	N/D	N/D
	peptidase_C58-like super family [b]; TM (CoVe4)	WP_006960006.1	VIC_RS11685	WP_006960006.1	G3U99_RS19905	WP_006960006.1	JV59_RS23695
	Unknown (CoVe5)	WP_006961218.1	VIC_RS16620	WP_165579899.1	G3U99_RS23535	WP_040121739.1	JV59_RS20315
	ADP-ribosyltransferase [b] (CoVe6)	WP_006961766.1	VIC_RS18765	WP_021457687.1	G3U99_RS21080	N/A	N/A
	Peptidase_26-like [b] (CoVe7)	WP_006962231.1	VIC_RS20705	N/D	N/D	N/D	N/D
	TM (CoVe8)	WP_006962597.1	VIC_RS22130	N/D	N/D	N/D	N/D
	Unknown (CoVe9)	N/A	N/A	WP_141650583.1	G3U99_RS19765	N/A	N/A
Unknown	Phage shock protein PspA	N/D	N/D	WP_021456780.1	G3U99_RS10060	N/D	N/D

N/A, no homolog is encoded in the genome; N/D, a homolog is encoded in the genome but not detected in the mass-spectrometry analysis; TM, transmembrane helix (according to phobius); [a], according to HHpred; [b], according to NCBI CDD

282   *T6SS2 effectors are novel anti-eukaryotic toxins*

283   Since most of the T6SS1 effectors we identified are homologs of previously described effectors,
284   we focused on the novel T6SS2 effectors for subsequent analyses. Altogether, the identified
285   *Vcor* T6SS2 effector repertoire comprises nine putative novel effectors, which we named
286   *Coralliilyticus* Virulence effector 1 to 9 (CoVe1-9): CoVe1, 2, 4, and 5 were identified in the
287   secretomes of all three strains; CoVe6 was identified in the secretomes of BAA-450 and
288   OCN008; CoVe3, 7, and 8 were identified only in the secretome of BAA-450; and CoVe9 was
289   identified only in the secretome of OCN008 (**Table 2**).

290   Six of the nine CoVes contain domains with predicted toxic activities (**Table 2**), including
291   peptidase [51], ADP-ribosyltransferase [53], cytotoxic necrotizing factor (CNF)-like deamidase
292   [54], and (p)ppGpp synthetase/hydrolase [55]. However, CoVe5, 8, and 9 sequence analyses
293   did not reveal significant similarity to any previously investigated toxin, suggesting that they
294   harbor novel toxic domains.

295   We sought to investigate these putative effectors. First, we set out to further validate their
296   T6SS2-dependent secretion using a standard secretion assay. To this end, we cloned the nine
297   putative effectors (CoVe1-8 from strain BAA-450 and CoVe9 from strain OCN008) into an
298   arabinose-inducible expression plasmid, fused to a C-terminal FLAG tag, and monitored their
299   secretion to the media from *Vcor* strains. As shown in **Fig. S3**, T6SS2-dependent secretion of all
300   CoVes, except CoVe3, was evident upon ectopic over-expression from a plasmid in their
301   respective encoding *Vcor* strain. Since CoVe3 T6SS2-dependent secretion was observed in the
302   more sensitive comparative proteomics approach when endogenously expressed from the
303   bacterial chromosome (**Fig. 6**), it is possible that its over-expression from a plasmid hampered
304   the secretion; alternatively, the C-terminal tag that we added to allow CoVe immunoblot
305   detection may have interfered with CoVe3 secretion.

306   Next, we tested our hypothesis that these novel effectors target eukaryotes. In support of this
307   hypothesis, we found that all nine effectors are toxic when ectopically expressed from a
308   galactose-inducible plasmid in a eukaryotic heterologous model organism, the yeast
309   *Saccharomyces cerevisiae* [56,57] (**Fig. 7A**). In contrast, these effectors were not toxic when
310   expressed from an arabinose-inducible plasmid in *E. coli*, used as a surrogate model bacterium
311   (**Fig. 7B** and **Fig. S4**). These results indicate that T6SS2 secretes an arsenal of novel effectors
312   with anti-eukaryotic activities.
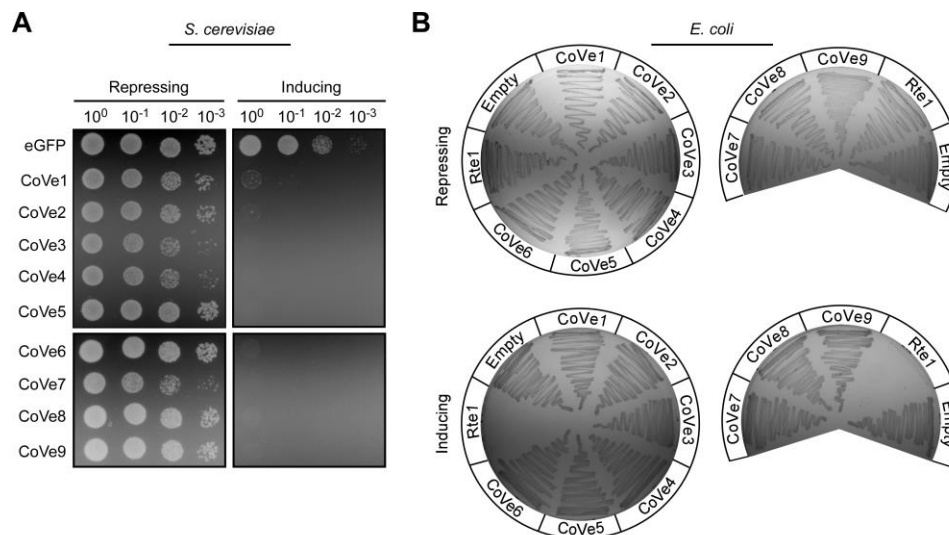
313 **Fig. 7.** *Vibrio coralliilyticus* **T6SS2 effectors are toxic in eukaryotic cells. A)** CoVes are
314 toxic in yeast. Tenfold serial dilutions of *Saccharomyces cerevisiae* strains containing plasmids
315 for the galactose-inducible expression of the indicated CoVes, or eGFP used as a negative
316 control, were spotted on repressing (2% [wt/vol] glucose) or inducing (2% [wt/vol] galactose and
317 1% [wt/vol] raffinose) agar plates. eGFP, enhanced GFP. **(B)** CoVes are not toxic to bacteria.
318 *Escherichia coli* strains containing plasmids for the arabinose-inducible expression of the
319 indicated, C-terminally FLAG-tagged CoVes, the *V. campbellii* antibacterial T6SS effector Rte1
320 used as a positive control, or an empty plasmid (Empty) were streaked onto repressing (0.4%
321 [wt/vol] glucose) or inducing (0.001% [wt/vol] arabinose) agar plates. Results from a
322 representative experiment out of at least three independent experiments are shown.

323

324 *T6SS2 effectors are differentially distributed in Vibrio coralliilyticus genomes*

325 We and others previously showed that T6SS effector repertoires can be divided into core
326 effectors present in all strains harboring the system and accessory effectors encoded only by a
327 subset of strains [25,58,59]. Therefore, we sought to determine the distribution of CoVes in *Vcor*
328 genomes. Interestingly, seven of the nine CoVes are found in all available RefSeq *Vcor*
329 genomes (**Fig. 8** and **Dataset S6**). We propose that these seven CoVes constitute the core
330 effector repertoire of the *Vcor* T6SS2. In contrast, two effectors, CoVe6 and CoVe9, are found
331 only in a subset of strains, suggesting that they are part of the accessory T6SS2 effector
332 repertoire. Interestingly, homologs of CoVe2 and CoVe8 are also found in all *Vcor* genomes
333 (**Fig. S2** and **Dataset S6**). Even though these homologs were not identified in our comparative
334 proteomics analyses, it is possible that they are also T6SS2 effectors.
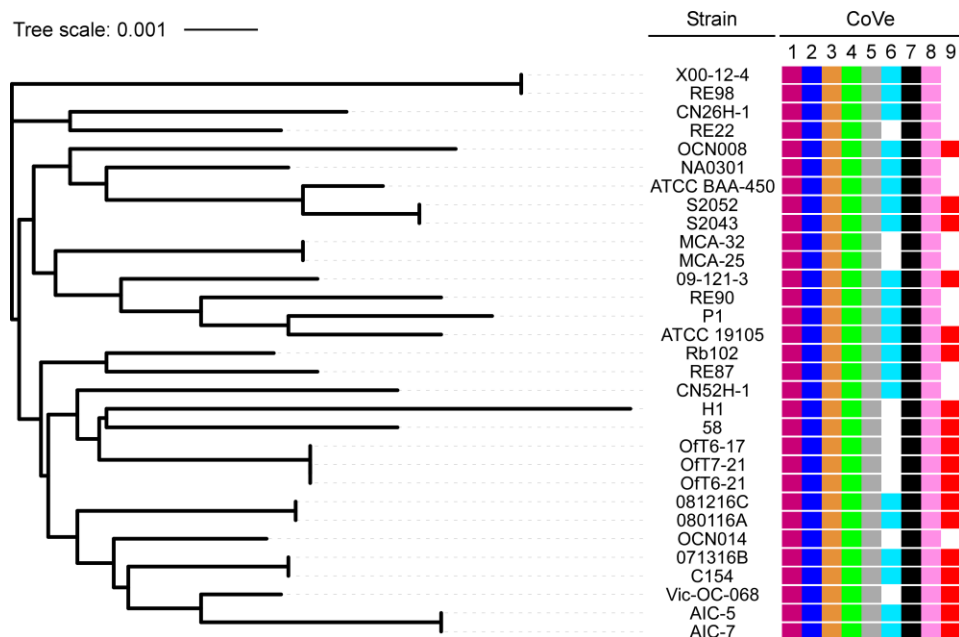
335 **Fig. 8. The *Vibrio coralliilyticus* T6SS2 effector repertoire can be divided into core and**
336 **accessory arsenals.** Distribution of T6SS2 CoVe1-9 effectors in RefSeq *Vcor* genomes. The
337 phylogenetic tree is based on DNA sequences of *rpoB*, coding for DNA-directed RNA
338 polymerase subunit β. The evolutionary history was inferred using the neighbor-joining method.

339

Discussion

Vibrio coralliilyticus (*Vcor*) is a pathogen that inflicts devastating ecological and economic losses. Although environmental conditions, such as high temperatures, have been associated with increased virulence and a pathogenic lifestyle, the exact virulence factors it uses remain poorly understood. Here, we systematically analyzed the T6SSs in the *Vcor* pan-genome. We revealed two omnipresent T6SSs, T6SS1 and T6SS2, which are regulated by temperature and appear to contribute to *Vcor* virulence. Whereas T6SS1 mediates antibacterial toxicity and thus possibly contributes to host colonization indirectly, T6SS2 secretes an array of novel anti-eukaryotic effectors and appears to play a direct role in virulence.

T6SS1 plays a role in interbacterial competition, possibly contributing to the elimination of host microbiota during host colonization. The T6SS1 effectors identified in our comparative proteomics analyses are homologs of effectors previously reported in similar T6SSs of other vibrios [22,28,45,60] or that have been predicted based on the presence of the MIX domain that defines a widespread class of polymorphic T6SS effectors [22,45]. Therefore, we did not investigate these effectors further in this work.

A recent report implicated prophage induction by LodAB-mediated hydrogen peroxide production as a mechanism *Vcor* uses to outcompete non-pathogenic competitors in the host [61]. Although it is plausible that such competition is mediated by a combination of contact-independent mechanisms, such as the abovementioned prophage induction, and contact-dependent mechanisms, such as the T6SS1-mediated competition, the *Vcor* strains investigated in our study lack LodAB homologs. Moreover, an Orthologous average nucleotide identity (orthoANI) analysis suggested that the SCSIO 43001 strain containing LodAB does not belong to the *Vcor* species (**Dataset S1**). Therefore, we propose that the omnipresent, antibacterial T6SS1 plays a major role in the ability of pathogenic *Vcor* strains to colonize their host.

T6SS2 secretes an array of anti-eukaryotic effectors and mediates toxicity during infection of a model host, *Artemia* nauplii, and during infection of macrophages. Because T6SS2 is induced at high temperatures, in correlation with the onset of *Vcor* virulence, we propose that it plays a role in the colonization and toxicity towards its natural hosts, coral and shellfish larvae. In future work, we will investigate the contribution of T6SS2 to *Vcor*'s virulence in these natural hosts, and we will also determine whether it targets the coral itself or its endosymbiotic dinoflagellates.

Notably, only a few anti-eukaryotic T6SS effectors are known [35,36]. Although we recently revealed anti-eukaryotic effectors in vibrios, belonging to the RIX effector class [42], the CoVes do not belong to any known polymorphic effector class and appear to be new T6SS effectors that have not been previously described. Even though their activities and cellular targets remain to be investigated, six CoVes harbor putative catalytic domains that have previously been implicated in virulence. Future investigations will reveal their mechanism of action and target inside eukaryotic cells.

Although we did not observe T6SS2 secretion in the poor GASW media in *Vcor* OCN008, this system contributed to this strain's virulence during the infection of *Artemina* nauplii. Because the *Artemia* infection assays were also performed in poor media (i.e., Instant Ocean), an unknown host factor possibly contributes to the system's activation during infection. Notably, our results suggest that additional factors contribute to the virulence towards *Artemia*, since inactivation of T6SS2 did not completely abolish toxicity in this host. Interestingly, the results of the BMDM infection assays indicate that the *Vcor* T6SS2 is also active at high temperatures of 37°C, which are infrequent in marine environments. It appears that under these conditions, the anti-eukaryotic toxicity of *Vcor* strains is mediated predominantly by T6SS2, since its inactivation abrogated toxicity to BMDMs. This observation suggests that *Vcor* might also be virulent to

13

388 warm-blooded organisms, although, at this time, we have no direct evidence to support this
389 hypothesis.

390

Materials and Methods

392 **Strains and media:** For a complete list of strains used in this study, see **Table S1**. *Escherichia*
393 *coli* strain DH5α (λ-pir) was grown in 2xYT broth (1.6% [wt/vol] tryptone, 1% [wt/vol] yeast
394 extract, and 0.5% [wt/vol] NaCl) or on Lysogeny broth (LB) agar plates (1.5% [wt/vol]) at 37°C.
395 The media were supplemented with chloramphenicol (10 µg/ml) to maintain plasmids when
396 needed. To repress expression from arabinose-inducible P*bad* promoters, 0.4% (wt/vol) D-
397 glucose was added to the media. To induce expression from P*bad*, L-arabinose was added to
398 the media at 0.001 or 0.1% (wt/vol), as indicated.

399 *Vibrio coralliilyticus* (*Vcor*) strains ATCC BAA-450, OCN008 and OCN014, and their derivatives
400 were grown in Marine Lysogeny broth (MLB; LB containing 3% [wt/vol] NaCl) or on GASW-Tris
401 agar plates (20.8 [g/l] NaCl, 0.56 [g/l] KCl, 4.8 [g/l] $MgSO_4 \cdot 7H_2O$, 4 [g/l] $MgCl_2 \cdot 6H_2O$, 0.01 [g/l]
402 K_2HPO_4, 0.001 [g/l] $FeSO_4 \cdot 7H_2O$, 2 [g/l] Instant Ocean sea salts, 6.33 [g/l] Tris base [$C_4H_{11}NO_3$],
403 4 [g/l] tryptone, 2 [g/l] yeast extract, 0.2% [vol/vol] glycerol, and 1.5% [wt/vol] agar; pH was
404 adjusted to 8.3 with HCl) at 30°C. For colony selection after plasmid conjugation (see below),
405 *Vcor* was grown on TCBS agar (Millipore, #86348) plates. L-arabinose (0.01% [wt/vol]) was
406 added to the media to induce expression from P*bad*.

407 *Vibrio natriegens* ATCC 14048 were grown on Marine Minimal Media (MMM) agar plates (2%
408 [wt/vol] NaCl, 0.4% [wt/vol] galactose, 5 mM $MgSO_4$, 7 mM K_2SO_4, 77 mM K_2HPO_4, 35 mM
409 KH_2PO_4, 2 mM NH_4Cl, and 1.5% [wt/vol] agar) at 30°C. The media were supplemented with
410 chloramphenicol (10 µg/ml) to select for or maintain plasmids when necessary.

411 *Saccharomyces cerevisiae* were grown in Yeast Extract–Peptone–Dextrose broth (YPD; 1%
412 [wt/vol] yeast extract, 2% [wt/vol] peptone, and 2% [wt/vol] glucose) or on YPD agar plates (2%
413 [wt/vol]) at 30°C. Yeast containing plasmids that provide prototrophy to leucine were grown in
414 Synthetic Dropout media (SD; 6.7 [g/l] yeast nitrogen base without amino acids, 1.4 [g/l] yeast
415 synthetic dropout medium supplement (Sigma)) supplemented with histidine (2 [ml/l] from a 1%
416 [wt/vol] stock solution), tryptophan (2 [ml/l] from a 1% [wt/vol] stock solution), uracil (10 [ml/l]
417 from a 0.2% [wt/vol] stock solution), and glucose (4% [wt/vol]). For galactose-inducible
418 expression from a plasmid, cells were grown in SD media or on SD agar plates supplemented
419 with galactose (2% [wt/vol]) and raffinose (1% [wt/vol]).

420 **Plasmid construction:** For a complete list of plasmids used in this study, see **Table S2**. For a
421 complete list of primers used in this study, see **Table S3**. To enable strong, arabinose-inducible
422 protein expression in *Vcor*, we constructed the plasmid pKara1. To this end, we amplified the
423 region between the *araC* cassette and *rrnB* T1 terminator, including a C-terminally FLAG-tagged
424 sfGFP gene, from the plasmid psfGFP [60], and introduced it 220 bp upstream of the gene
425 encoding the fluorescent protein DsRed in pVSV208 [62], using the Gibson assembly method.

426 For expression in bacteria, the coding sequences (CDS) of the indicated genes of interest were
427 amplified by PCR from the respective genomic DNA of the encoding bacterium. Next, amplicons
428 were inserted into the multiple cloning site (MCS) of pBAD33.1^F, or in place of the sfGFP gene
429 within pKara1, using the Gibson assembly method [63], in-frame with the C-terminal FLAG tag.
430 Plasmids were introduced into *E. coli* DH5α (λ-pir) by electroporation and into vibrios via
431 conjugation. Transconjugants were selected on TCBS agar (Millipore) plates supplemented with
432 chloramphenicol and then counter-selected on GASW agar plates containing chloramphenicol.

14

433 For galactose-inducible expression in yeast, genes were inserted into the MCS of the shuttle
434 vector pGML10 (Riken) using the Gibson assembly method, in-frame with a C-terminal Myc tag.
435 Yeast transformations were performed using the lithium acetate method, as described
436 previously [64].

437 **Construction of deletion strains:** To delete genes in *Vcor* BAA-450, OCN008, and OCN014,
438 1 kb sequences upstream and downstream of each gene to be deleted were cloned together
439 into the MCS of pDM4, a $Cm^R OriR6K$ suicide plasmid. The pDM4 constructs were transformed
440 into *E. coli* DH5α (λ-pir) by electroporation and then conjugated into *Vcor* strains.
441 Transconjugants were selected on TCBS agar plates supplemented with chloramphenicol and
442 then counter-selected on agar plates containing 15% (wt/vol) sucrose for loss of the *sacB*-
443 containing plasmid. Deletions were confirmed by PCR.

444 *Vibrio* **protein secretion assays:** Secretion and expression assays were performed as
445 previously reported [24], with minor modifications. *Vcor* strains were grown for 16 hours in MLB
446 supplemented with antibiotics to maintain plasmids when necessary. Bacterial cultures were
447 diluted four-fold in fresh media and incubated for two additional hours at 28°C. Then, the
448 cultures were normalized to an optical density at 600 nm (OD_{600}) of 0.18 in 5 ml of MLB or
449 GASW media, as indicated. When protein expression from an arabinose-inducible plasmid was
450 required, the media were supplemented with chloramphenicol and 0.01% (wt/vol) L-arabinose.
451 The cultures were then incubated with continuous shaking (220 rpm) at 19°C, 23°C, 28°C or
452 31°C, as indicated, for four hours. For expression fractions, 0.5 OD_{600} units were harvested, and
453 cell pellets were resuspended in 30 μl of 2x Tris-glycine SDS sample buffer (Novex, Life
454 Sciences) with 5% (vol/vol) β-mercaptoethanol. For secretion fractions, supernatant volumes
455 equivalent to 5 OD_{600} units were filtered (0.22 μm), and proteins were precipitated using the
456 deoxycholate and trichloroacetic acid method [65]. The precipitated proteins were washed twice
457 with cold acetone and air-dried before being resuspended in 20 μl of 100 mM Tris-Cl (pH = 8.0)
458 and 20 μl of 2x Tris-glycine SDS sample buffer containing 5% (vol/vol) β-mercaptoethanol.
459 Protein samples were incubated at 95°C for 10 minutes before being resolved on TGX Stain-
460 free gels (Bio-Rad). The proteins were transferred onto 0.2 μm nitrocellulose membranes using
461 Trans-Blot Turbo Transfer (Bio-Rad), following the manufacturer's protocol. Membranes were
462 then immunoblotted with custom-made α-Hcp2 (GenScript; polyclonal antibodies raised in
463 rabbits against the peptides CGEGGKIEKGPEVGF or CVMTKPNREGSGADP; the latter was
464 used only in the experiment shown in Fig. 2A), Custom-made polyclonal α-VgrG1 [66],
465 monoclonal α-FLAG (Sigma-Aldrich, F1804), or Direct-Blot^{TM} HRP anti-*E. coli* RNA polymerase
466 sigma 70 (mouse mAb #663205; BioLegend; referred to as α-RNAP) antibodies at a dilution of
467 1:1000. Protein signals were detected using enhanced chemiluminescence (ECL) reagents with
468 a Fusion FX6 imaging system (Vilber Lourmat).

469 **Mass spectrometry analyses:** Sample preparations for mass spectrometry were performed as
470 described in the "*Vibrio* protein secretion assays" section. After the acetone wash step, samples
471 were shipped to the Smoler Proteomics Center at the Technion, Israel, for analysis. Precipitated
472 proteins were washed twice in 80% (vol/vol) cold acetone. The protein pellets were dissolved in
473 8.5 M Urea, 400 mM ammonium bicarbonate, and 10 mM DTT. Protein concentrations were
474 estimated using the Bradford assay. The proteins were reduced at 60ºC for 30 minutes and then
475 modified with 35.2 mM iodoacetamide in 100 mM ammonium bicarbonate for 30 minutes at
476 room temperature in the dark. The proteins were digested overnight at 37ºC in 1.5 M urea and
477 66 mM ammonium bicarbonate with modified trypsin (Promega) at a 1:50 (M/M) enzyme-to-
478 substrate ratio. An additional trypsinization step was performed for four hours. The resulting
479 tryptic peptides were analyzed by LC-MS/MS using Q Exactive HF mass spectrometer (Thermo)
480 fitted with a capillary HPLC (Evosep). The peptides were loaded onto a 15 cm ID 150 1.9-
481 micron (Batch no. E1121-3-24) column of Evosep. The peptides were eluted with the built-in

15

482 Xcalibur 15 SPD (88 min) method. Mass spectrometry was performed in a positive mode using
483 repetitively full MS scan (m/z 350–1200) followed by High energy Collision Dissociation (HCD)
484 of the 20 most dominant ions selected from the full MS scan. A dynamic exclusion list was
485 enabled with exclusion duration of 20 seconds.

486 The mass spectrometry data were analyzed with the MaxQuant software 2.1.1.0
487 (www.maxquant.org) using the Andromeda search engine [67] against the relevant *Vcor* strains
488 from the Uniprot database, with a mass tolerance of 4.5 ppm for the precursor masses and 4.5
489 ppm for the fragment ions. Peptide- and protein-level false discovery rates (FDRs) were filtered
490 to 1% using the target-decoy strategy. The protein table was filtered to eliminate identities from
491 the reverse database and common contaminants. The data were quantified by label-free
492 analysis using the same software, based on extracted ion currents (XICs) of peptides, enabling
493 quantitation from each LC/MS run for each peptide identified in any of the experiments.
494 Statistical analyses of the identification and quantization results were done using the Perseus
495 1.6.7.0 software [68]. The mass spectrometry proteomics data have been deposited in the
496 ProteomeXchange Consortium via PRIDE [69].

497 **Bacterial competition assays:** Bacterial competition assays were performed as previously
498 described [24], with minor modifications. Attacker and prey strains were grown for 16 hours in
499 appropriate media. In the morning, *Vcor* attacker strains were diluted 1:10 into fresh media and
500 incubated for an additional hour at 28°C. Attacker and prey cultures were then normalized to an
501 OD_{600} of 0.5 and mixed at a 4:1 (attacker:prey) ratio in triplicate. Next, the mixtures were spotted
502 (25 µl) on MLB agar competition plates and incubated at 28°C for 4 h. The colony-forming units
503 (CFU) of the prey strains at t = 0 h were determined by plating tenfold serial dilutions on
504 selective media plates. After 4 hours of co-incubation on competition plates, the bacteria were
505 harvested, and the CFUs of the surviving prey strains were determined as described above.
506 Prey strains contained a pBAD33.1 plasmid to allow selective growth on plates containing
507 chloramphenicol.

508 ***Vibrio coralliilyticus* growth assays:** Triplicates *Vcor* cultures grown for 16 hours were
509 normalized to OD_{600} = 0.01 in MLB and transferred to a 96-well plate (200 µl per well). The 96-
510 well plate was incubated in a microplate reader (BioTek SYNERGY H1) at 28°C with continuous
511 shaking (205 cpm). Growth was measured as OD_{600} in 10-minute intervals.

512 ***Artemia* infection assays:** *Artemia* infection assays were performed as previously reported
513 [41], with minor modifications. *Artemia salina* eggs (Artemio Pur; JBL) were incubated in
514 deionized distilled water containing chloramphenicol (10 µg/ml), kanamycin (100 µg/ml), and
515 ampicillin (100 µg/ml) at 28°C with continuous rotation for an hour. The eggs were washed four
516 times with Instant Ocean solution (3.3% [wt/vol]; Aquarium Systems) and then incubated for 24
517 hours with continuous rotation at 28°C. Hatched *Artemia* nauplii were transferred into sterile 48-
518 well plates (two nauplii per well in 400 µl Instant Ocean). Approximately 5×10^{7} bacteria were
519 added to each well, and the plates were incubated at 28°C under 12-hour light and dark cycles.
520 *Artemia* survival was determined at the indicated timepoints post-infection. An *Artemia* nauplius
521 that did not move for 10 seconds was defined as non-viable. Each bacterial strain was added to
522 8 wells (16 nauplii). Survival results are provided as grouped data from four independent
523 experiments. Percent survival was calculated as surviving subjects out of the subjects at risk for
524 each time point.

525 **BMDM infection assays:** Bone marrow cells from 6-8 week-old mice were isolated, and bone
526 marrow-derived macrophages (BMDMs) were obtained after a 7-day differentiation, as
527 previously described [70]. *Vcor* strains were grown for 16 hours in MLB. In the morning,
528 bacterial cultures were diluted tenfold into fresh media and incubated for an additional hour at
529 28°C. Approximately 3.5×10^{4} BMDMs were seeded into 96-well plates in triplicates in 1%

530 (vol/vol) FBS and penicillin-streptomycin-free DMEM media and then infected with the
531 indicated *Vcor* strains at a multiplicity of infection (MOI) ~ 4. Plates were centrifuged for 5
532 minutes at 400 x *g*. Propidium iodide (PI; 1 µg/ml) was added to the medium 30 minutes prior to
533 infection, and its uptake kinetics were assessed every 15 minutes using real-time microscopy
534 (Incucyte SX5) during incubation at 37°C. The data were analyzed using the Incucyte SX5
535 analysis software and exported to Graphpad PRISM. Normalization was performed according to
536 the maximal PI-positive object count to calculate the percentage of dead cells [70].

537 **Yeast toxicity assays:** Toxicity assays in yeast were performed as previously described [64].
538 Briefly, yeast cells were cultured for 16 hours in SD media supplemented with 4% glucose
539 (wt/vol). Bacterial cultures were washed twice with sterile deionized distilled water and
540 normalized to an OD_{600} of 1.0 in sterile deionized water. Then, tenfold serial dilutions were
541 spotted onto SD agar plates containing 4% (wt/vol) glucose (repressing plates) or 2% (wt/vol)
542 galactose and 1% (wt/vol) raffinose (inducing plates). The plates were incubated at 28°C for two
543 days.

544 **Protein expression in *E. coli*:** Overnight-grown bacterial cultures of *E. coli* DH5α (λ-pir) strains
545 carrying pBAD33.1 arabinose-inducible expression plasmids were grown in 2xYT broth
546 supplemented with chloramphenicol. Bacterial cultures were normalized to an OD_{600} = 0.5 in 3
547 ml fresh 2xYT with chloramphenicol and incubated with continuous shaking (220 rpm) at 37°C
548 for 2 hours. Then, L-arabinose was added to a final concentration of 0.1% (wt/vol) to induce
549 protein expression, and the cultures were incubated for two additional hours. Cells equivalent to
550 0.5 OD_{600} units were harvested, and their pellets were resuspended in 50 µl of 2x Tris-glycine
551 SDS sample buffer (Novex, Life Sciences) supplemented with 5% (vol/vol) β-mercaptoethanol.
552 Subsequently, the samples were boiled at 95°C for 10 minutes and resolved on a TGX stain-free
553 gel (Bio-Rad) for SDS-PAGE analysis. The proteins were transferred onto nitrocellulose
554 membranes, which were then immunoblotted with α-FLAG (Sigma-Aldrich, F1804) antibodies at
555 a 1:1000 dilution. Finally, protein signals were detected using ECL in a Fusion FX6 imaging
556 system (Vilber Lourmat). The loading control for total protein lysates was visualized as the
557 fluorescence of activated trihalo compounds found in the gel.

558 *E. coli* **toxicity assays:** To determine the toxicity of *Vcor* proteins in bacteria, *E. coli* DH5α (λ-
559 pir) strains carrying pBAD33.1 arabinose-inducible expression plasmids were streaked onto LB
560 agar plates supplemented with chloramphenicol and either 0.4% (wt/vol) glucose (repressing
561 plates) or 0.001% (wt/vol) L-arabinose (inducing plates). Plates were incubated for 16 hours at
562 37°C.

563 **Identifying T6SS gene clusters in *Vibrio coralliilyticus*:** A local database containing the
564 RefSeq bacterial nucleotide and protein sequences was generated (last updated on August 21,
565 2023). *Vcor* genomes were retrieved from the local database, and OrthoANI [71] was performed
566 as described previously [72]. The *Vcor* strain SCSIO 43001 genome (assembly accession
567 GCF_024449095.1) was removed from the dataset because it showed OrthoANI values <95%.
568 The *Vcor* strain RE22 (assembly accession GCF_001297935.1) was removed because an
569 updated version of strain RE22 was found (assembly accession GCF_003391375.1).

570 The presence of T6SS gene clusters in *Vcor* genomes was determined by following a two-step
571 procedure described previously [50]. Briefly, in the first step, BLASTN was employed to align
572 *Vcor* nucleotide sequences against the nucleotide sequences of representative T6SS clusters
573 (**Fig. 1** and **Dataset S2**). The best alignments for each nucleotide accession number were
574 saved. In the second step, a two-dimensional matrix was generated for each T6SS gene cluster.
575 The matrices were filled in with the percent identity values based on the positions of the
576 alignments from the first step. The overall coverage was calculated for each T6SS gene cluster

577 in each genome. *Vcor* genomes with at least 70% overall coverage of a T6SS gene cluster were
578 regarded as containing that T6SS gene cluster (**Dataset S2**).

579 **Identifying effector homologs in *Vibrio coralliilyticus* genomes:** BLASTP was employed to
580 identify homologs of the T6SS2 effectors in *Vcor* genomes, as described previously [25]. The
581 amino acid sequences of new CoVes from strains BAA-450 (WP_006957348.1,
582 WP_006959328.1, WP_006959836.1, WP_006960006.1, WP_006961218.1, WP_006961766.1,
583 WP_006962231.1, and WP_006962597.1) and OCN008 (WP_141650583.1) were used as
584 queries. The E-value threshold was set to $10^{-12,}$ and the coverage was set to 70% based on the
585 length of the query sequences.

586 **Constructing a phylogenetic tree:** The nucleotide sequences of the *rpoB* gene, coding for
587 DNA-directed RNA polymerase subunit beta, were retrieved from the local RefSeq database.
588 Phylogenetic analyses of bacterial genomes were conducted using the MAFFT 7 server
589 (mafft.cbrc.jp/alignment/server/) as described before [73]. A multiple sequence alignment was
590 generated using MAFFT v7 FFT-NS-I [74,75]. The evolutionary history of *Vcor* genomes was
591 inferred using the neighbor-joining method [76] with the Jukes-Cantor substitution model (JC69).
592 The analysis included 31 nucleotide sequences and 4,029 conserved sites.

593

Data Availability

595 The mass spectrometry proteomics data have been deposited in the ProteomeXchange
596 Consortium via the PRIDE [69] partner repository with the dataset identifier PXD049479.

597

Conflict of Interest

599 The authors declare no competing interests.

600

Acknowledgments

609

Author contributions

611 Conceptualization: BU, JvK, and DS; Formal Analysis: SM, HC, EB, and DS; Funding
612 Acquisition: MG, BU, JvK, EB, and DS; Investigation: SM, HC, and EB; Methodology: SM, HC,
613 and EB; Resources: MG, BU, JvK; Supervision: DS; Writing – Original Draft Preparation: SM
614 and DS; Writing – Review and Editing: HC, MG, BU, JvK, and EB.

615

References

617 1. Horseman MA, Bray R, Lujan-Francis B, Matthew E. Infections Caused by Vibrionaceae.
618   Infect Dis Clin Pract. 2013;21: 222–232. doi:10.1097/IPC.0b013e3182826328

619 2. Baker-Austin C, Oliver JD, Alam M, Ali A, Waldor MK, Qadri F, et al. Vibrio spp.
620   infections. Nat Rev Dis Prim. 2018;4: 1–19. doi:10.1038/s41572-018-0005-8

621 3. Martinez-Urtaza J, Baker-Austin C, Jones JL, Newton AE, Gonzalez-Aviles GD, DePaola
622   A. Spread of Pacific Northwest *Vibrio parahaemolyticus* Strain. N Engl J Med. 2013;369:
623   1573–1574. doi:10.1056/NEJMc1305535

624 4. Le Roux F, Wegner KM, Baker-Austin C, Vezzulli L, Osorio CR, Amaro C, et al. The
625   emergence of Vibrio pathogens in Europe: Ecology, evolution and pathogenesis (Paris,
626   11-12 March 2015). Front Microbiol. 2015;6: 1–8. doi:10.3389/fmicb.2015.00830

627 5. Vezzulli L, Grande C, Reid PC, Hélaouët P, Edwards M, Höfle MG, et al. Climate
628   influence on *Vibrio* and associated human diseases during the past half-century in the
629   coastal North Atlantic. Proc Natl Acad Sci. 2016;113: E5062–E5071.
630   doi:10.1073/pnas.1609157113

631 6. Newton A, Kendall M, Vugia DJ, Henao OL, Mahon BE. Increasing Rates of Vibriosis in
632   the United States, 1996–2010: Review of Surveillance Data From 2 Systems. Clin Infect
633   Dis. 2012;54: S391–S395. doi:10.1093/cid/cis243

634 7. Burke S, Pottier P, Lagisz M, Macartney EL, Ainsworth T, Drobniak SM, et al. The impact
635   of rising temperatures on the prevalence of coral diseases and its predictability: A global
636   meta-analysis. Ecol Lett. 2023;26. doi:10.1111/ele.14266

637 8. Arboleda M, Reichardt W. Epizoic communities of prokaryotes on healthy and diseased
638   scleractinian corals in Lingayen Gulf, Philippines. Microb Ecol. 2009;57.
639   doi:10.1007/s00248-008-9400-0

640 9. Moriarty T, Leggat W, Huggett MJ, Ainsworth TD. Coral Disease Causes, Consequences,
641   and Risk within Coral Restoration. Trends in Microbiology. 2020.
642   doi:10.1016/j.tim.2020.06.002

643 10. Elliff CI, Silva IR. Coral reefs as the first line of defense: Shoreline protection in face of
644   climate change. Marine Environmental Research. 2017.
645   doi:10.1016/j.marenvres.2017.03.007

646 11. Mera H, Bourne DG. Disentangling causation: complex roles of coral-associated
647   microorganisms in disease. Environmental Microbiology. 2018. doi:10.1111/1462-
648   2920.13958

649 12. Bender-Champ D, Diaz-Pulido G, Dove S. Effects of elevated nutrients and CO2
650   emission scenarios on three coral reef macroalgae. Harmful Algae. 2017;65.
651   doi:10.1016/j.hal.2017.04.004

652 13. Vanwonterghem I, Webster NS. Coral Reef Microorganisms in a Changing Climate.
653   iScience. 2020. doi:10.1016/j.isci.2020.100972

654 14. Tout J, Siboni N, Messer LF, Garren M, Stocker R, Webster NS, et al. Increased
655   seawater temperature increases the abundance and alters the structure of natural Vibrio
656   populations associated with the coral Pocillopora damicornis. Front Microbiol. 2015;6.
657   doi:10.3389/fmicb.2015.00432

658 15. Ben-Haim Y, Zicherman-Keren M, Rosenberg E. Temperature-regulated bleaching and
659   lysis of the coral Pocillopora damicornis by the novel pathogen Vibrio coralliilyticus. Appl
660   Environ Microbiol. 2003;69: 4236–42. Available:
661   http://www.ncbi.nlm.nih.gov/pubmed/12839805

662 16. Ushijima B, Videau P, Burger AH, Shore-Maggio A, Runyon CM, Sudek M, et al. Vibrio

663   coralliilyticus strain OCN008 is an etiological agent of acute montipora white syndrome.
664   Appl Environ Microbiol. 2014;80. doi:10.1128/AEM.03463-13

665   17.   Richards GP, Watson MA, Needleman DS, Church KM, Häse CC. Mortalities of Eastern
666   And Pacific oyster larvae caused by the pathogens Vibrio coralliilyticus and Vibrio
667   tubiashii. Appl Environ Microbiol. 2015;81. doi:10.1128/AEM.02930-14

668   18.   Ushijima B, Richards GP, Watson MA, Schubiger CB, Häse CC. Factors affecting
669   infection of corals and larval oysters by Vibrio coralliilyticus. PLoS One. 2018;13.
670   doi:10.1371/journal.pone.0199475

671   19.   Kimes NE, Grim CJ, Johnson WR, Hasan NA, Tall BD, Kothary MH, et al. Temperature
672   regulation of virulence factors in the pathogen Vibrio coralliilyticus. ISME J. 2012;6: 835–
673   846. doi:10.1038/ismej.2011.154

674   20.   Childers BM, Klose KE. Regulation of virulence in Vibrio cholerae: The ToxR regulon.
675   Future Microbiology. 2007. doi:10.2217/17460913.2.3.335

676   21.   Ushijima B, Videau P, Poscablo D, Stengel JW, Beurmann S, Burger AH, et al. Mutation
677   of the toxR or mshA genes from Vibrio coralliilyticus strain OCN014 reduces infection of
678   the coral Acropora cytherea. Environ Microbiol. 2016;18. doi:10.1111/1462-2920.13428

679   22.   Dar Y, Salomon D, Bosis E. The antibacterial and anti-eukaryotic Type VI secretion
680   system MIX-effector repertoire in Vibrionaceae. Mar Drugs. 2018;16: 433.
681   doi:10.1016/bs.ctdb.2015.10.001

682   23.   Pukatzki S, Ma AT, Sturtevant D, Krastins B, Sarracino D, Nelson WC, et al. Identification
683   of a conserved bacterial protein secretion system in Vibrio cholerae using the
684   Dictyostelium host model system. Proc Natl Acad Sci. 2006;103: 1528–1533.
685   doi:10.1073/pnas.0510322103

686   24.   Salomon D, Gonzalez H, Updegraff BL, Orth K. Vibrio parahaemolyticus Type VI
687   secretion system 1 Is activated in marine conditions to target bacteria, and is differentially
688   regulated from system 2. PLoS One. 2013;8: e61086. doi:10.1371/journal.pone.0061086

689   25.   Tchelet D, Keppel K, Bosis E, Salomon D. Vibrio parahaemolyticus T6SS2 effector
690   repertoires. Gut Microbes. 2023;15. doi:10.1080/19490976.2023.2178795

691   26.   Salomon D, Klimko JA, Trudgian DC, Kinch LN, Grishin N V., Mirzaei H, et al. Type VI
692   secretion system toxins horizontally shared between marine bacteria. PLoS Pathog.
693   2015;11: 1–20. doi:10.1371/journal.ppat.1005128

694   27.   Speare L, Cecere AG, Guckes KR, Smith S, Wollenberg MS, Mandel MJ, et al. Bacterial
695   symbionts use a type VI secretion system to eliminate competitors in their natural host.
696   Proc Natl Acad Sci U S A. 2018;115: E8528–E8537. doi:10.1073/pnas.1808302115

697   28.   Ray A, Schwartz N, Souza Santos M, Zhang J, Orth K, Salomon D, et al. Type VI
698   secretion system MIX-effectors carry both antibacterial and anti-eukaryotic activities.
699   EMBO Rep. 2017;18: e201744226. doi:10.15252/embr.201744226

700   29.   Piel D, Bruto M, James A, Labreuche Y, Lambert C, Janicot A, et al. Selection of Vibrio
701   crassostreae relies on a plasmid expressing a type 6 secretion system cytotoxic for host
702   immune cells. Environ Microbiol. 2020;22. doi:10.1111/1462-2920.14776

703   30.   Wang J, Brodmann M, Basler M. Assembly and subcellular localization of bacterial type
704   VI secretion systems. Annu Rev Microbiol. 2019;73. doi:10.1146/annurev-micro-020518-
705   115420

706   31.   Jana B, Salomon D. Type VI secretion system: a modular toolkit for bacterial dominance.

20

707   Future Microbiol. 2019;14: fmb-2019-0194. doi:10.2217/fmb-2019-0194

708   32. Hernandez RE, Gallegos-Monterrosa R, Coulthurst SJ. Type VI secretion system effector
709   proteins: Effective weapons for bacterial competitiveness. Cellular Microbiology. 2020.
710   doi:10.1111/cmi.13241

711   33. Allsopp LP, Bernal P. Killing in the name of: T6SS structure and effector diversity.
712   Microbiology. 2023;169: 001367. doi:10.1099/MIC.0.001367

713   34. Basler M, Pilhofer M, Henderson GP, Jensen GJ, Mekalanos JJ. Type VI secretion
714   requires a dynamic contractile phage tail-like structure. Nature. 2012;483: 182–6.
715   doi:10.1038/nature10846

716   35. Hachani A, Wood TE, Filloux A. Type VI secretion and anti-host effectors. Curr Opin
717   Microbiol. 2016;29: 81–93. doi:10.1016/j.mib.2015.11.006

718   36. Monjarás Feria J, Valvano MA. An Overview of Anti-Eukaryotic T6SS Effectors. Frontiers
719   in Cellular and Infection Microbiology. 2020. doi:10.3389/fcimb.2020.584751

720   37. Huang Y, Du P, Zhao M, Liu W, Du Y, Diao B, et al. Functional characterization and
721   conditional regulation of the type VI secretion system in Vibrio fluvialis. Front Microbiol.
722   2017;8: 1–15. doi:10.3389/fmicb.2017.00528

723   38. MacIntyre DL, Miyata ST, Kitaoka M, Pukatzki S. The Vibrio cholerae type VI secretion
724   system displays antimicrobial properties. Proc Natl Acad Sci. 2010;107: 19520–19524.
725   doi:10.1073/pnas.1012931107

726   39. Church SR, Lux T, Baker-Austin C, Buddington SP, Michell SL. Vibrio vulnificus type 6
727   secretion system 1 contains anti-bacterial properties. PLoS One. 2016;11: 1–17.
728   doi:10.1371/journal.pone.0165500

729   40. Cohen H, Baram N, Fridman CM, Edry-Botzer L, Salomon D, Gerlic M. Post-
730   phagocytosis activation of NLRP3 inflammasome by two novel T6SS effectors. Elife.
731   2022;11: e82766.

732   41. Cohen H, Fridman CM, Gerlic M, Salomon D. A Vibrio T6SS-Mediated Lethality in an
733   Aquatic Animal Model. Cascales E, editor. Microbiol Spectr. 2023;11.
734   doi:10.1128/spectrum.01093-23

735   42. Kanarek K, Fridman CM, Bosis E, Salomon D. The RIX domain defines a class of
736   polymorphic T6SS effectors and secreted adaptors. Nat Commun 2023 141. 2023;14: 1–
737   13. doi:10.1038/s41467-023-40659-2

738   43. Bruto M, James A, Petton B, Labreuche Y, Chenivesse S, Alunno-Bruscia M, et al. Vibrio
739   crassostreae, a benign oyster colonizer turned into a pathogen after plasmid acquisition.
740   ISME J. 2017;11: 1043–1052. doi:10.1038/ismej.2016.162

741   44. Guillemette R, Ushijima B, Jalan M, Häse CC, Azam F. Insight into the resilience and
742   susceptibility of marine bacteria to T6SS attack by Vibrio cholerae and Vibrio
743   coralliilyticus. PLoS One. 2020;15. doi:10.1371/journal.pone.0227864

744   45. Salomon D, Kinch LN, Trudgian DC, Guo X, Klimko JA, Grishin N V., et al. Marker for
745   type VI secretion system effectors. Proc Natl Acad Sci. 2014;111: 9271–9276.
746   doi:10.1073/pnas.1406110111

747   46. Ben-Haim Y, Thompson FL, Thompson CC, Cnockaert MC, Hoste B, Swings J, et al.
748   Vibrio coralliilyticus sp. nov., a temperature-dependent pathogen of the coral Pocillopora
749   damicornis. Int J Syst Evol Microbiol. 2003;53. doi:10.1099/ijs.0.02402-0

21

47. Ushijima B, Videau P, Poscablo D, Vine V, Salcedo M, Aeby G, et al. Complete genome sequence of Vibrio coralliilyticus strain OCN014, isolated from a diseased coral at Palmyra Atoll. Genome Announc. 2014;2. doi:10.1128/genomeA.01318-14

48. Neu AK, Månsson M, Gram L, Prol-García MJ. Toxicity of bioactive and probiotic marine bacteria and their secondary metabolites in artemia sp. and caenorhabditis elegans as eukaryotic model organisms. Appl Environ Microbiol. 2014;80. doi:10.1128/AEM.02717-13

49. Austin B, Austin D, Sutherland R, Thompson F, Swings J. Pathogenicity of vibrios to rainbow trout (Oncorhynchus mykiss, Walbaum) and Artemia nauplii. Environ Microbiol. 2005;7: 1488–1495. doi:10.1111/j.1462-2920.2005.00847.x

50. Jana B, Keppel K, Fridman CM, Bosis E, Salomon D. Multiple T6SSs, mobile auxiliary modules, and effectors revealed in a systematic analysis of the Vibrio parahaemolyticus pan-genome. Bordenstein S, editor. mSystems. 2022; e00723-22. doi:10.1128/MSYSTEMS.00723-22

51. Iriarte M, Cornelis GR. YopT, a new Yersinia Yop effector protein, affects the cytoskeleton of host cells. Mol Microbiol. 1998;29. doi:10.1046/j.1365-2958.1998.00992.x

52. Teufel F, Almagro Armenteros JJ, Johansen AR, Gíslason MH, Pihl SI, Tsirigos KD, et al. SignalP 6.0 predicts all five types of signal peptides using protein language models. Nat Biotechnol. 2022;40. doi:10.1038/s41587-021-01156-3

53. Deng Q, Barbieri JT. Molecular mechanisms of the cytotoxicity of ADP-ribosylating toxins. Annual Review of Microbiology. 2008. doi:10.1146/annurev.micro.62.081307.162848

54. Knust Z, Schmidt G. Cytotoxic necrotizing factors (CNFs)-a growing toxin family. Toxins. 2010. doi:10.3390/toxins2010116

55. Ahmad S, Wang B, Walker MD, Tran HKR, Stogios PJ, Savchenko A, et al. An interbacterial toxin inhibits target cell growth by synthesizing (p)ppApp. Nature. 2019;575: 674–678. doi:10.1038/s41586-019-1735-9

56. Siggers KA, Lesser CF. The Yeast Saccharomyces cerevisiae: A Versatile Model System for the Identification and Characterization of Bacterial Virulence Proteins. Cell Host Microbe. 2008;4: 8–15. doi:10.1016/j.chom.2008.06.004

57. Popa C, Coll NS, Valls M, Sessa G. Yeast as a Heterologous Model System to Uncover Type III Effector Function. Bliska JB, editor. PLOS Pathog. 2016;12: e1005360. doi:10.1371/journal.ppat.1005360

58. Robinson LA, Collins ACZ, Murphy RA, Davies JC, Allsopp LP. Diversity and prevalence of type VI secretion system effectors in clinical Pseudomonas aeruginosa isolates. Front Microbiol. 2023;13. doi:10.3389/fmicb.2022.1042505

59. Unterweger D, Miyata ST, Bachmann V, Brooks TM, Mullins T, Kostiuk B, et al. The Vibrio cholerae type VI secretion system employs diverse effector modules for intraspecific competition. Nat Commun. 2014;5: 3549. doi:10.1038/ncomms4549

60. Dar Y, Jana B, Bosis E, Salomon D. A binary effector module secreted by a type VI secretion system. EMBO Rep. 2022;23: e53981. doi:10.15252/embr.202153981

61. Wang W, Tang K, Wang P, Zeng Z, Xu T, Zhan W, et al. The coral pathogen Vibrio coralliilyticus kills non-pathogenic holobiont competitors by triggering prophage induction. Nat Ecol Evol 2022 68. 2022;6: 1132–1144. doi:10.1038/s41559-022-01795-y

62. Dunn AK, Millikan DS, Adin DM, Bose JL, Stabb E V. New *rfp*- and pES213-derived tools

for analyzing symbiotic *Vibrio fischeri* reveal patterns of infection and *lux* expression in situ. Appl Environ Microbiol. 2006;72: 802–810. doi:10.1128/AEM.72.1.802-810.2006

63. Gibson DG, Young L, Chuang RY, Venter JC, Hutchison CA, Smith HO. Enzymatic assembly of DNA molecules up to several hundred kilobases. Nat Methods. 2009;6: 343–345. doi:10.1038/nmeth.1318

64. Salomon D, Sessa G. Identification of growth inhibition phenotypes induced by expression of bacterial type III effectors in yeast. J Vis Exp. 2010; 4–7. doi:10.3791/1865

65. Bensadoun A, Weinstein D. Assay of proteins in the presence of interfering materials. Anal Biochem. 1976;70: 241–250. doi:10.1016/S0003-2697(76)80064-4

66. Li P, Kinch LN, Ray A, Dalia AB, Cong Q, Nunan LM, et al. Acute hepatopancreatic necrosis disease-causing Vibrio parahaemolyticus strains maintain an antibacterial type VI secretion system with versatile effector repertoires. Appl Environ Microbiol. 2017;83: e00737-17. doi:10.1128/AEM.00737-17

67. Cox J, Hein MY, Luber CA, Paron I, Nagaraj N, Mann M. Accurate proteome-wide label-free quantification by delayed normalization and maximal peptide ratio extraction, termed MaxLFQ. Mol Cell Proteomics. 2014;13. doi:10.1074/mcp.M113.031591

68. Tyanova S, Temu T, Sinitcyn P, Carlson A, Hein MY, Geiger T, et al. The Perseus computational platform for comprehensive analysis of (prote)omics data. Nature Methods. 2016. doi:10.1038/nmeth.3901

69. Perez-Riverol Y, Bai J, Bandla C, García-Seisdedos D, Hewapathirana S, Kamatchinathan S, et al. The PRIDE database resources in 2022: A hub for mass spectrometry-based proteomics evidences. Nucleic Acids Res. 2022;50. doi:10.1093/nar/gkab1038

70. Erlich Z, Shlomovitz I, Edry-Botzer L, Cohen H, Frank D, Wang H, et al. Macrophages, rather than DCs, are responsible for inflammasome activity in the GM-CSF BMDC model. Nature Immunology. 2019. doi:10.1038/s41590-019-0313-5

71. Lee I, Ouk Kim Y, Park S-C, Chun J. OrthoANI: An improved algorithm and software for calculating average nucleotide identity. Int J Syst Evol Microbiol. 2016;66: 1100–1103. doi:10.1099/ijsem.0.000760

72. Fridman CM, Keppel K, Gerlic M, Bosis E, Salomon D. A comparative genomics methodology reveals a widespread family of membrane-disrupting T6SS effectors. Nat Commun. 2020;11: 1085. doi:10.1038/s41467-020-14951-4

73. Jana B, Fridman CM, Bosis E, Salomon D. A modular effector with a DNase domain and a marker for T6SS substrates. Nat Commun. 2019;10: 3595. doi:10.1038/s41467-019-11546-6

74. Katoh K, Misawa K, Kuma K, Miyata T. MAFFT: a novel method for rapid multiple sequence alignment based on fast Fourier transform. Nucleic Acids Res. 2002;30: 3059–66. Available: http://www.ncbi.nlm.nih.gov/pubmed/12136088

75. Katoh K, Rozewicki J, Yamada KD. MAFFT online service: Multiple sequence alignment, interactive sequence choice and visualization. Brief Bioinform. 2018;20: 1160–1166. doi:10.1093/bib/bbx108

76. Saitou N, Nei M. The neighbor-joining method: a new method for reconstructing phylogenetic trees. Mol Biol Evol. 1987;4: 406–425. doi:10.1093/oxfordjournals.molbev.a040454